

# ON OUTAGE PROBABILITY AND THROUGHPUT PERFORMANCE OF COGNITIVE RADIO INSPIRED NOMA RELAY SYSTEM

Thanh-Nam TRAN<sup>1</sup>, Dinh-Thuan DO<sup>2</sup>, Miroslav VOZNAK<sup>1</sup>

<sup>1</sup>Department of Telecommunications, Faculty of Electrical Engineering and Computer Science, VSB–Technical University of Ostrava, 17. listopadu 15, 708 00 Ostrava, Czech Republic

<sup>2</sup>Department of Electronics and Telecommunications, Faculty of Electronics Technology, Industrial University of Ho Chi Minh City, 12 Nguyen Van Bao, Go Vap, Ho Chi Minh City, Vietnam

thanh.nam.tran.st@vsb.cz, dodinhthuan@iuh.edu.vn, miroslav.voznak@vsb.cz

DOI: 10.15598/aece.v16i4.2801

**Abstract.** To improve the throughput and the outage probability of the Cognitive Radio (CR) inspired system, a novel Non-Orthogonal Multiple Access (NOMA) can be deployed to adapt multiple services in 5G wireless communication. In this scheme, after the reception of the superposition coded symbol with a predefined power allocation factors from the primary source, the relay decodes and forwards with a new superposition coded symbol (i.e. allocating another power factors) to the destination. By employing twin antenna design at the relay, the bandwidth efficiency in such scheme will be improved. Assuming Rayleigh fading channels, the closed-form expressions in terms of throughput and the outage performance are derived. Through numerical results, they showed that the outage performance of the proposed scheme using a Single Antenna (SA) scheme at the relay is better than a Twin Antenna (TA) scheme because SA scheme is not affected by its own antenna interference.

## Keywords

**CR-NOMA, NOMA system, outage probability, single antenna, throughput, twin antenna.**

## 1. Introduction

The physical connection technology in mobile networks are called Radio Access Network (RAN). By allocating a subcarrier for many users in the same time, Non-Orthogonal Multiple Access (NOMA) has higher throughput than Orthogonal Frequency Division Multiple Access (OFDMA) [1]. Therefore, NOMA

promises to become the future mobile network technology. In particular, the next-generation (5G) network has a higher requirement for system performance in terms of throughput and bandwidth efficiency. By using the superimposed signal at the transmitter and the continuous noise cancellation at the receiver [2] and [3], NOMA provides higher spectral efficiency. In a NOMA system, to improve capacity, Successive Interference Cancellation (SIC) is used. For downlink transmissions, by using different power factors, the source can transmit multiplexed signals for multiple destinations over the same subcarrier. The source detects the received signals at each destination. The first destination has the best Signal to Noise Ratio (SNR) which is successfully decoded by using the SIC. The best quality signal is regenerated by extracting its own symbol from the received complex signal [4].

Regarding recent advance in NOMA, the coverage extend can be addressed by using relaying networks in NOMA with respect to enhanced outage performance and capacity as investigations in [5] and [6]. The authors in [7] further apply the NOMA principle to a Multiple-Input Single-Output (MISO) system, and solve the downlink sum rate maximization problem. To consider a more practical situation, [8] proposes full-duplex relay which decodes received symbols and simultaneously sends a superimposed composite signal to the destinations.

In other line of research as in [9] and [10], energy harvesting assisted system model are introduced as potential source to prolong lifetime of such wireless networks. Cooperative Simultaneous Wireless Information and Power Transfer (SWIPT) NOMA protocol was proposed in [11], in which the NOMA-strong users are considered as energy harvesting relays to help the

NOMA-weak users. Closed-form expressions for sum-throughput and outage probability with static powers for different users for the uplink NOMA system were derived in [12]. Additionally, the joint Antenna Selection (AS) scheme can be proposed in multiple antenna cognitive radio-inspired NOMA network such as in [13], where the authors introduced an algorithm to optimize the signal-to-noise ratio as examining the secondary user performance adapt to under the quality of service for the primary user.

To improve spectrum efficiency is the paradigm of underlay Cognitive Radio (CR) networks, which was proposed in [14] and has rekindled increasing interest in using the spectrum more efficiently. The key idea of underlay CR networks is that each secondary user is allowed to access the spectrum of the primary users as long as the secondary meets a certain interference threshold in the primary network. In [15], an underlay CR network taking into account the spatial distribution of the secondary user relays and primary users were considered, and its performance was evaluated by using stochastic geometry tools. Motivated by above analysis, especially [8] and [15], we explore outage and throughput performance of potential CR-inspired NOMA scheme. The main contribution of this paper relies in idea of CR-NOMA opportunistically serving the primary user on the condition that the secondary user's Quality of Service (QoS) is guaranteed.

The rest of this paper is organized as follows. Section 2. presents the system model of CR-NOMA. In Sec. 3. , we perform the performance system analysis. Section 4. examines the analysis and simulation results. Finally, Sec. 5. completes with conclusion remarks for the paper and reviews the important results.

## 2. System Models of CR-NOMA

In this paper, a downlink wireless transmitter system consists of a primary source and a number of User Equipments (UEs). Relays are operated in full-duplex modes and the destinations have only one antenna. In such proposed schemes, relays in the CR-NOMA system are equipped with a twin antenna or a single antenna.

In practice, NOMA can be considered as a special scenario of CR systems [15]. In such CR-NOMA, a primary user with poor channel conditions is assigned to same spectrum sharing with secondary users who are with strong channel conditions. The main reason to deploy CR-NOMA is that the QoS requirement is guaranteed for the weak users.

For simplicity in the following analysis, Primary Source, Primary Relay 1, Secondary Relay 2, Primary Destination 1, and Secondary Destination 2 are denoted as  $PS$ ,  $PR1$ ,  $SR2$ ,  $PD1$  and  $SD2$ , respectively. In addition, we assumed that channels between the  $PS$  transmitting to  $PR1$  and  $SR2$  are two independent random variables following a complex Gaussian distribution with zero mean and variances, i.e.,  $h_{S,R1} \sim CN(0, \sigma_{S,R1}^2)$ ,  $h_{S,R2} \sim CN(0, \sigma_{S,R2}^2)$ . Each of UEs can either function as a terminal device or a relay. In NOMA system, the case of poor signal quality, the system requires a relay for forwarding the signal. In particular, when the signal channels from  $PS$  to  $PD1$  and  $SD2$  are poor, in this case, two others UEs (so-called relay) which obtain strong signals, are used for dual-hop cooperative transmission.  $P_S$  is the transmission power of the  $PS$ . It can be assumed in NOMA, the selected channel arrangement is required as  $|h_{S,R1}|^2 > |h_{S,R2}|^2$ .

### 2.1. CR-NOMA Using a TA Scheme

Figure 2 is an illustration of CR-NOMA using a Twin Antenna (TA) scheme at each of the relays for bandwidth efficiency enhancement. To complete a transmission round, two time slots are necessary to transmit a signal from  $PS$  to the destinations  $PD$  and  $SD$ . In the First Time Slot (FTS),  $PS$  sends a mixed signal  $S_S^{TA} = (\sqrt{\alpha_S}P_S M_1 + \sqrt{\beta_S}P_S M_2)$ , where  $M_1$  and  $M_2$  are the incoming signals for  $PD1$  and  $SD1$ , respectively. The power factors for  $PD1$  and  $SD2$  are the sum of both  $\alpha_S$  and  $\beta_S$ , where  $\alpha_S + \beta_S = 1$ .

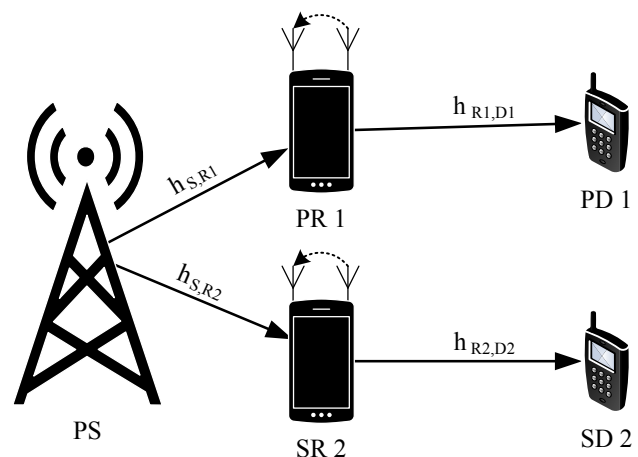


Fig. 1: The CR-NOMA using a TA scheme.

At relay,  $PR1$  receives a signal following expression as:

$$y_{R1}^{TA} = h_{S,R1} \left( \sqrt{\alpha_S}P_S M_1 + \sqrt{\beta_S}P_S M_2 \right) + h_{LI,R1} \sqrt{\omega_{R1}P_{R1}} I_{LI,R1} + n_{S,R1}. \tag{1}$$

Similarly, the signal received at relay  $SR2$  is

$$y_{R2}^{TA} = h_{S,R2} \left( \sqrt{\alpha_S P_S} M_1 + \sqrt{\beta_S P_S} M_2 \right) + h_{LI,R2} \sqrt{\omega_{R2} P_{R2}} I_{LI,R2} + n_{S,R2}, \quad (2)$$

where  $n_{S,Ri}$ ,  $i \in \{1, 2\}$ , is Additive White Gaussian Noise (AWGN) and following  $n_{S,i} \sim CN(0, N_0)$  and the residual loop self-interference ( $LI$ ) is modeled as a Rayleigh fading feedback channel with coefficient  $h_{LI,Ri}$ , where  $i \in \{1, 2\}$ . The received signals will be decoded by using SIC at both relays. In phase 1, for  $PR1$ ,  $M_2$  will be decoded by treating  $M_1$  as interference and  $M_2$  has the achievable Signal-to-Interference-plus-Noise Ratio (SINR) defined as:

$$\begin{aligned} \gamma_{R1,M2}^{TA} &= \frac{|h_{S,R1}|^2 \beta_S P_S}{|h_{S,R1}|^2 \alpha_S P_S + |h_{LI,R1}|^2 \omega_{R1} P_{R1} + N_0} \\ &= \frac{|h_{S,R1}|^2 \beta_S P_S}{|h_{S,R1}|^2 \alpha_S \rho_S + |h_{LI,R1}|^2 \omega_{R1} \rho_{R1} + 1}, \end{aligned} \quad (3)$$

$$\text{where } \rho_S = \frac{P_S}{N_0}, \rho_{R1} = \frac{P_{R1}}{N_0}.$$

In phase 2, after decoding  $M_2$ , relay  $PR1$  will then subtract  $M_2$  from the mixed signal with AWGN and  $LI$ . Therefore,  $M_1$  has the achievable SINR of

$$\begin{aligned} \gamma_{R1,M1}^{TA} &= \frac{|h_{S,R1}|^2 \alpha_S P_S}{|h_{LI,R1}|^2 \omega_{R1} P_{R1} + N_0} \\ &= \frac{|h_{S,R1}|^2 \alpha_S P_S}{|h_{LI,R1}|^2 \omega_{R1} \rho_{R1} + 1}. \end{aligned} \quad (4)$$

In the same way, at relay  $SR2$  for phase one,  $M_2$  will be decoded by treating  $M_1$  as interference and  $M_2$  has the achievable SINR as below:

$$\begin{aligned} \gamma_{R2,M2}^{TA} &= \frac{|h_{S,R2}|^2 \beta_S P_S}{|h_{S,R2}|^2 \alpha_S P_S + |h_{LI,R2}|^2 \omega_{R2} P_{R2} + N_0} \\ &= \frac{|h_{S,R2}|^2 \beta_S P_S}{|h_{S,R2}|^2 \alpha_S \rho_S + |h_{LI,R2}|^2 \omega_{R2} \rho_{R2} + 1}, \end{aligned} \quad (5)$$

where  $\rho_{R2} = \frac{P_{R2}}{N_0}$ , and in phase second, it subtracts  $M_2$  from the signals.

$$\begin{aligned} \gamma_{R2,M1}^{TA} &= \frac{|h_{S,R2}|^2 \alpha_S P_S}{|h_{LI,R2}|^2 \omega_{R2} P_{R2} + N_0} \\ &= \frac{|h_{S,R2}|^2 \alpha_S P_S}{|h_{LI,R2}|^2 \omega_{R2} \rho_{R2} + 1}. \end{aligned} \quad (6)$$

Then, the instantaneous rate at both of relays are

$$R_{Ri,Mi}^{TA} = \frac{1}{2} \log_2 (1 + \gamma_{Ri,Mi}^{TA}), \quad (7)$$

where  $i \in \{1, 2\}$ . And in the Second Time Slot (STS),  $PR1$  sent  $\bar{M}_1$  to  $PD1$ , while  $SR2$  was sending  $\bar{M}_2$  to

$SD2$ . The signals are received at  $PD1$  and  $SD1$  are presented as:

$$y_{D1}^{TA} = h_{R1,D1} \sqrt{\omega_{R1} P_{R1}} \bar{M}_1 + N_0, \quad (8)$$

and

$$y_{D2}^{TA} = h_{R2,D2} \sqrt{\omega_{R2} P_{R2}} \bar{M}_2 + N_0. \quad (9)$$

Therefore, SINRs for  $PD1$  and  $SD1$  can be written as

$$\begin{aligned} \gamma_{D1}^{TA} &= \frac{|h_{R1,D1}|^2 \omega_{R1} P_{R1}}{N_0} \\ &= |h_{R1,D1}|^2 \omega_{R1} \rho_{R1}, \end{aligned} \quad (10)$$

and

$$\begin{aligned} \gamma_{D2}^{TA} &= \frac{|h_{R2,D2}|^2 \omega_{R2} P_{R2}}{N_0} \\ &= |h_{R2,D2}|^2 \omega_{R2} \rho_{R2}. \end{aligned} \quad (11)$$

Achievable rate at both  $PD1$  and  $SD2$  are

$$R_{Di}^{TA} = \frac{1}{2} \log_2 (1 + \gamma_{Di}^{TA}), \quad (12)$$

where  $i \in \{1, 2\}$ .

## 2.2. CR-NOMA Using a SA Scheme

In this scheme, the  $PS$  sends a mixed signal  $S_S^{SA} = (\sqrt{\alpha_S P_S} M_1 + \sqrt{\beta_S P_S} M_2)$  to both of relays, where each of them has only one antenna and thus receives the signals without  $LI$ . In FTS, the received signals are expressed by Eq. (13).

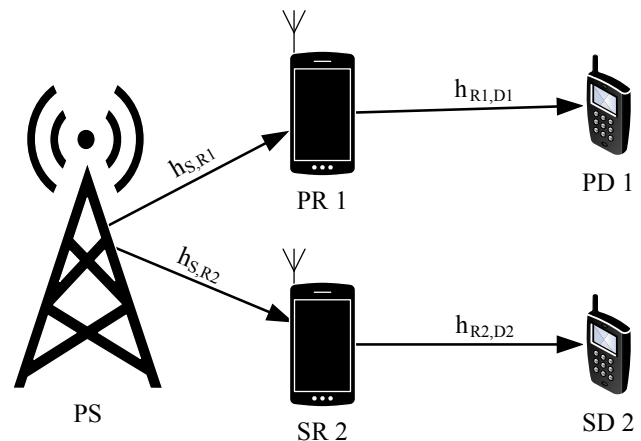


Fig. 2: CR-NOMA using a SA scheme.

$$y_{S,Ri}^{SA} = h_{S,Ri} \left( \sqrt{\alpha_S P_S} M_1 + \sqrt{\beta_S P_S} M_2 \right) + n_{S,Ri}, \quad (13)$$

where  $i \in \{1, 2\}$ .

These are decoded  $M_2$  by treating  $M_1$  and  $n_{S,Ri}$  as noise, and we have SNR as below:

$$\begin{aligned} \gamma_{Ri,M_2}^{SA} &= \frac{|h_{S,Ri}|^2 \beta_S P_S}{|h_{S,Ri}|^2 \alpha_S P_S + N_0} \\ &= \frac{|h_{S,Ri}|^2 \beta_S \rho_S}{|h_{S,Ri}|^2 \alpha_S \rho_S + 1}, \end{aligned} \tag{14}$$

and then, SNR is computed to decode  $M_1$ :

$$\begin{aligned} \gamma_{Ri,M_1}^{SA} &= \frac{|h_{S,Ri}|^2 \alpha_S P_S}{N_0} \\ &= |h_{S,Ri}|^2 \alpha_S \rho_S. \end{aligned} \tag{15}$$

Next, the achievable rates at both  $PR1$  and  $SR2$  are computed by

$$R_{Ri,M_i}^{SA} = \frac{1}{3} \log_2 (1 + \gamma_{Ri,M_i}^{SA}). \tag{16}$$

In the STS, the received signals at both destinations are expressed by  $y_{Di}^{SA}$  as:

$$y_{Di}^{SA} = h_{Ri,Di} \sqrt{\omega_{Ri} P_{Ri}} \bar{M}_i + n_{Ri,Di}, \tag{17}$$

where  $i \in \{1, 2\}$  and  $\omega_{Ri} = 1$ . That means the relay uses 100 % of the transmit power to transmit signals to the destinations.

By using available CSI, the signal is decoded which is denoted as  $\gamma_{Di}^{SA}$ , where  $i \in \{1, 2\}$ :

$$\gamma_{Di}^{SA} = \frac{|h_{Ri,Di}|^2 \omega_{Ri} P_{Ri}}{N_0} = |h_{Ri,Di}|^2 \omega_{Ri} \rho_{Ri}. \tag{18}$$

Therefore, the achievable rate at destination  $R_{Di}^{SA}$ , where  $i \in \{1, 2\}$ , can be expressed as

$$R_{Di}^{SA} = \frac{1}{3} \log_2 (1 + \gamma_{Di}^{SA}). \tag{19}$$

### 3. The Performance System Analysis

The performance of our proposed model is presented by the evaluation results as outage probability and system throughput, respectively.

#### 3.1. Outage Probability System Analysis

In this section, we investigate the outage probability of CR-NOMA with both TA and SA schemes. In addition, we propose using a portion of the power to generate the signal, and the remaining power is used for the purpose of energy harvesting.

#### 1) Outage Probability System of CR-NOMA Using a TA Scheme

The predefined value of minimum rates for  $PD1$ ,  $SD2$  are denoted as  $R_{\min 1}$  and  $R_{\min 2}$ , respectively. If the achievable data rate is less than the minimum data rate, an outage will occur.

**Proposition 1:** We denoted  $P_{O,D1}^{TA}$  as the event of the outage at  $PD1$  which is expressed by

$$\begin{aligned} P_{O,D1}^{TA} &= 1 - P_{D1}^{TA} \\ &= 1 - \Pr (\min \{R_{R1,M1}^{TA}, R_{D1}^{TA}\} > R_{\min 1} \\ &\quad \wedge \min \{R_{R1,M2}^{TA}, R_{R2,M2}^{TA}\} > R_{\min 2}) \\ &= 1 - (\min \{Q_1, Q_3\}) (Q_2) (Q_4) \end{aligned} \tag{20}$$

and the event of the outage at  $SD2$  is denoted  $P_{O,D2}^{TA}$ :

$$\begin{aligned} P_{O,D2}^{TA} &= 1 - P_{D2}^{TA} \\ &= 1 - \Pr (R_{R1,M1}^{TA} > R_{\min 1} \\ &\quad \wedge \min \{R_{R1,M2}^{TA}, R_{R2,M2}^{TA}, R_{D2}^{TA}\} > R_{\min 2}) \\ &= 1 - (\min \{Q_1, Q_3\}) (Q_4) (Q_5), \end{aligned} \tag{21}$$

where  $Q_1, Q_2, Q_3, Q_4$  and  $Q_5$  are given by Eq. (22), Eq. (23), Eq. (24), Eq. (25) and Eq. (26), respectively:

$$Q_1 = e^{-\left(\frac{x_1}{\psi_1}\right)} \frac{\psi_1}{\psi_1 + \chi_1 \omega_{R1} \rho_{R1} \sigma_{h_{LI,R1}}^2}, \tag{22}$$

$$Q_2 = e^{-\left(\frac{x_1}{\epsilon_{R1} \rho_{R1} \sigma_{h_{R1,D1}}^2}\right)}, \tag{23}$$

$$Q_3 = e^{-\left(\frac{x_2}{\psi_3}\right)} \frac{\psi_3}{\psi_3 + \chi_2 \omega_{R1} \rho_{R1} \sigma_{h_{LI,R1}}^2}, \tag{24}$$

$$Q_4 = e^{-\left(\frac{x_2}{\psi_4}\right)} \frac{\psi_4}{\psi_4 + \chi_2 \omega_{R2} \rho_{R2} \sigma_{h_{LI,R2}}^2}, \tag{25}$$

$$Q_5 = e^{-\left(\frac{x_2}{\epsilon_{R2} \rho_{R2} \sigma_{h_{R2,D2}}^2}\right)}, \tag{26}$$

#### 2) Outage Probability Analysis of CR-NOMA Scheme Using a SA Scheme

In order to evaluate system performance using SA at the relay, we can compute outage event as follows:

**Proposition 2:** In this scheme, the outage probability at  $PD1$  is expressed as:

$$\begin{aligned} P_{O,D1}^{SA} &= 1 - P_{D1}^{SA} \\ &= 1 - \Pr (\min \{R_{R1,M1}^{SA}, R_{D1}^{SA}\} > R_{\min 1} \\ &\quad \wedge \min \{R_{R1,M2}^{SA}, R_{R2,M2}^{SA}\} > R_{\min 2}) \\ &= 1 - (\min \{Q_1', Q_3'\}) (Q_2') (Q_4') \end{aligned} \tag{27}$$

and the outage probability at  $SD2$  is given by:

$$\begin{aligned} P_{O,D2}^{SA} &= 1 - P_{D2}^{SA} \\ &= 1 - \Pr(R_{R1,M1}^{SA} > R_{\min 1} \\ &\wedge \min\{R_{R1,M2}^{SA}, R_{R2,M2}^{SA}, R_{D2}^{SA}\} > R_{\min 2}) \\ &= 1 - (\min\{Q_1', Q_3'\})(Q_4')(Q_5'), \end{aligned} \quad (28)$$

where  $Q_1', Q_2', Q_3', Q_4'$  and  $Q_5'$  are given by Eq. (29), Eq. (30), Eq. (31), Eq. (32) and Eq. (33) as below:

$$Q_1' = e^{-\left(\frac{x_1}{\alpha_S \rho_S \sigma_{h,S,R1}^2}\right)}, \quad (29)$$

$$Q_2' = e^{-\left(\frac{x_1}{\rho_{R1} \sigma_{d,R1,D1}^2}\right)}, \quad (30)$$

$$Q_3' = e^{-\left(\frac{x_2}{(\beta_S - x_2 \alpha_S) \rho_S \sigma_{h,S,R1}^2}\right)}, \quad (31)$$

$$Q_4' = e^{-\left(\frac{x_2}{(\beta_S - x_2 \alpha_S) \rho_S \sigma_{h,S,R2}^2}\right)}, \quad (32)$$

$$Q_5' = e^{-\left(\frac{x_1}{\rho_{R1} \sigma_{h,R2,D2}^2}\right)}. \quad (33)$$

### 3.2. Throughput Analysis

In this section, we analyze the throughput of  $TA$  and  $SA$  scheme. The throughput performance of CR-NOMA using a  $TA$  scheme is  $P_{D1+D2}^{TA}$  which is expressed as:

$$P_{D1+D2}^{TA} = (1 - P_{O,D1}^{TA}) R_{\min 1} + (1 - P_{O,D2}^{TA}) R_{\min 2}. \quad (34)$$

And the throughput performance of CR-NOMA using a  $SA$  scheme is  $P_{D1+D2}^{SA}$  which is computed as

$$P_{D1+D2}^{SA} = (1 - P_{O,D1}^{SA}) R_{\min 1} + (1 - P_{O,D2}^{SA}) R_{\min 2}. \quad (35)$$

### 3.3. The Proposed Power Reallocation at Relays

At both destinations, the received signals are expressed as:

$$y_{Di} = h_{Ri,Di} \sqrt{P_{Ri}} \bar{M}_i + n_i, \quad (36)$$

where  $i \in \{1, 2\}$ . Thus, SNR each of destination is expressed as:

$$\gamma_{Di} = \frac{|h_{Ri,Di}|^2 P_{Ri}}{N_0} = |h_{Ri,Di}|^2 \rho_{Ri}, \quad (37)$$

where  $i \in \{1, 2\}$ .

We propose various power factors at  $PR1$  and  $SR2$  which were  $\Delta_{R1}$  and  $\Delta_{R2}$  respectively. Instead of using 100 % of the transmit power, excess power  $(1 - \Delta_{R1})$ ,

where  $i \in \{1, 2\}$ , is used to transmit the energy to the receiver. Therefore, the signals received at  $PR1$  and  $SR2$  are expressed as:

$$\begin{aligned} y_{D1}^{EH} &= h_{R1,D1} \left( \sqrt{\Delta_{R1}} P_{R1} \bar{M}_1 \right. \\ &\quad \left. + \sqrt{(1 - \Delta_{R1}) P_{R1}} \Theta \right) + n_1, \end{aligned} \quad (38)$$

and

$$\begin{aligned} y_{D2}^{EH} &= h_{R2,D2} \left( \sqrt{\Delta_{R2}} P_{R2} \bar{M}_2 \right. \\ &\quad \left. + \sqrt{(1 - \Delta_{R2}) P_{R2}} \Theta \right) + n_2, \end{aligned} \quad (39)$$

where  $\Delta_{R1} = \alpha_S$ ,  $\Delta_{R2} = \beta_S$  and  $\Theta$  is a silent signal.

At  $PD1$ , the received signal which is decoded by extracting  $n_1$  and then we compute SNR as:

$$\gamma_{D1}^{EH} = \frac{|h_{R1,D1}|^2 \Delta_{R1} P_{R1}}{N_0} = |h_{R1,D1}|^2 \Delta_{R1} \rho_{R1}, \quad (40)$$

and

$$\gamma_{D2}^{EH} = \frac{|h_{R2,D2}|^2 \Delta_{R2} P_{R2}}{N_0} = |h_{R2,D2}|^2 \Delta_{R2} \rho_{R2}. \quad (41)$$

Similarly,  $PD1$  and  $SD2$  can be obtained the achievable rates as

$$R_{Di}^{EH} = \frac{1}{2} \log_2 \left( 1 + |h_{Ri,Di}|^2 \Delta_{Ri} \rho_{Ri} \right). \quad (42)$$

## 4. Numerical Results

In this section, we perform the analysis and simulation for both models. Firstly, this study provides valuable evaluations and simulations regarding on the outage probability and hence these proposed models demonstrate the quality of the system. It is important to notice that the system with the lower outage probability has better performance, and the higher throughput has better performance as well. The outage probability results and the few important parameters of the system are presented below.

Figure 3 shows the achieved outage probability by our proposed system models with  $\alpha_S = 0.2$ ,  $\beta_S = 0.8$ ,  $R_{\min 1} = R_{\min 2} = 0.5 \text{ b}\cdot\text{s}^{-1}\cdot\text{Hz}^{-1}$ , channel gains are set as  $\sigma_{S,R1}^2 = 5$ ,  $\sigma_{S,R2}^2 = 1$ ,  $\sigma_{Ri,Di}^2 = 1$ , where  $i \in \{1, 2\}$ ,  $\sigma_{S,D1}^2 = 0.5$ ,  $\sigma_{S,D2}^2 = 0.1$ , and the transmission SNRs of the  $PS$  from 0 dB to 50 dB to compare the outage probability of two models, namely SA and TA versus NOMA without relay in [2]. Moreover, Fig. 3 shows that the SA scheme has better performance than the TA scheme for all values of transmit SNR at the source due to existence of self-interference in TA. With the increasing level of transmitting SNRs, the outage performance of these schemes will be enhanced and

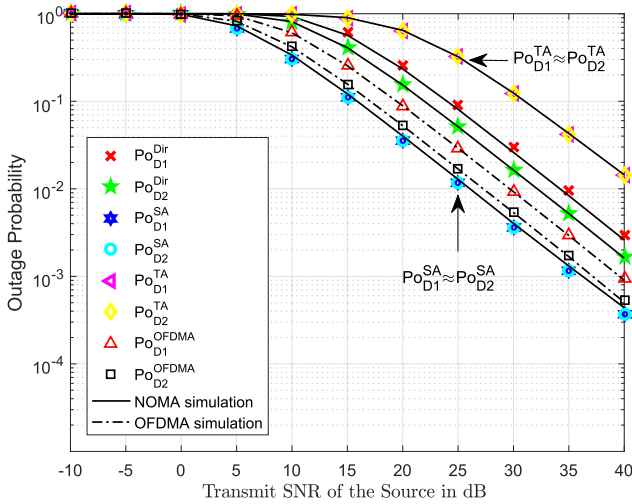


**Fig. 3:** Comparison of the outage probability of CR-NOMAs with other schemes.

hardly improves even at high SNR. Such phenomenon can be explained by the fact that the outage performance greatly depends on the power for signal processing. The performance gap of three schemes will be clearer at very high value of transmit SNR. Because the probabilities of  $Po_{D1}^{SA} \approx Po_{D2}^{SA}$  and  $Po_{D1}^{TA} \approx Po_{D2}^{TA}$  have approximately the same result. Therefore, we do not present individual results for subsequent results. The paired  $Po_{D1}^{SA}, Po_{D2}^{SA}$  and  $Po_{D1}^{TA}, Po_{D2}^{TA}$  will be expressed by  $Po_{D1,D2}^{SA}$  and  $Po_{D1,D2}^{TA}$  for the next formulas, respectively. In addition, the *PD1* and *SD2* have good outage probability results in the OFDMA scheme, which were denoted as  $Po_{D1}^{OFDMA}$  and  $Po_{D2}^{OFDMA}$ , respectively. However, these results, outage performance of  $Po_{D1}^{OFDMA}$  and  $Po_{D2}^{OFDMA}$  are worse compared to the results of NOMA system with SA relay, namely  $Po_{D1,D2}^{SA}$ . To ensure that the comparison is objective, we apply the same simulation parameters as in all proposed schemes.

Figure 4 illustrates the throughput of the CR-NOMA, in two modes regarding antenna architecture at the relay and the SNR threshold from 0 dB to 50 dB, below the threshold for outage,  $R_{th} = 0.5 \text{ b}\cdot\text{s}^{-1}\cdot\text{Hz}^{-1}$ . The results show that the SA scheme can achieve superior throughput performance to the TA scheme. In addition, it outperforms both the OFDMA and the direct link schemes. In particular, SA model with EH, which was denoted as  $P_{D1+D2}^{SA,EH}$ , also gives a decent system quality compared to other models, except for SA model without EH. As a result, both TA with EH and TA with EH schemes have the worst throughput. However, these results can be improved by increasing the transmit SNRs.

Next, we perform a system performance evaluation by comparing the outage probability of the SA and TA

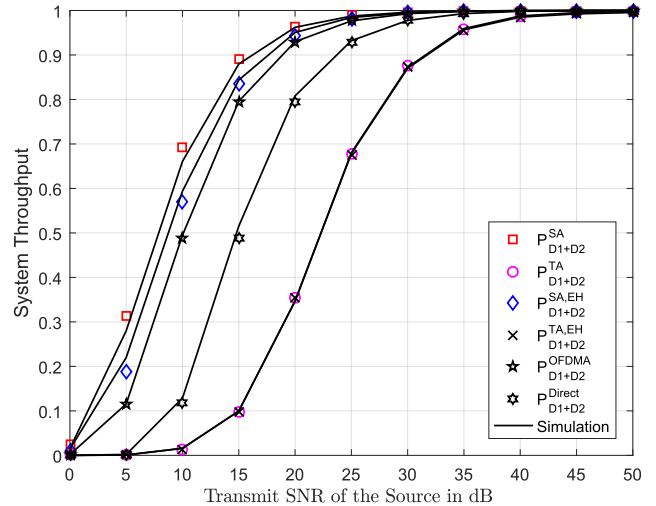


**Fig. 4:** The throughput results of CR-NOMA TA and SA schemes versus TA with EH, SA with EH, and OFDMA schemes.

scheme versus the SA with EH and TA with EH scheme which we proposed.

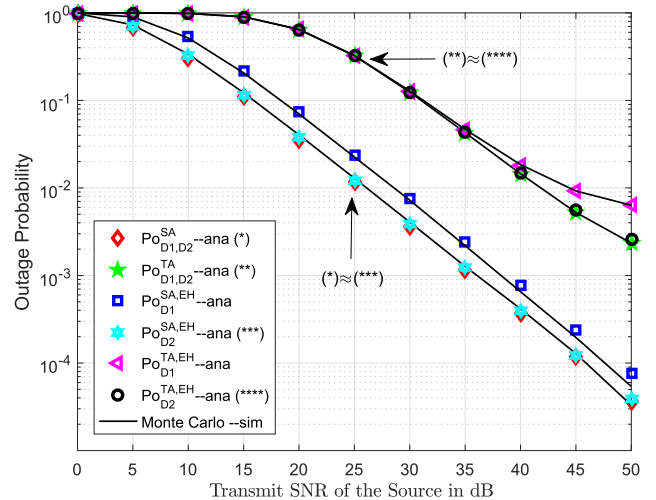


**Fig. 5:** Comparison study on the outage probability results of CR-NOMA using SA and TA schemes with EH.

In Fig. 5, the outage probability results of both *PD1* and *SD2* in SA and TA schemes, respectively, remain the same as in Fig. 3. We also investigate the outage probability analysis of *PD1* and *SD2* in SA and EH, TA and EH at the relays. The outage probability results of both SA with EH and TA with EH, namely  $Po_{Di}^{SA,EH}$  and  $Po_{Di}^{TA,EH}$ , showed that they are worse than without EH. But these results still guarantee QoS to the end user without having to use 100 % of the transmit power at the relay.

In Fig. 3, the outage probability results of *PD1* and *SD2* in TA scheme are worse than other results in other schemes, e.g. SA, SA and EH, OFDMA schemes. Therefore, the results in TA scheme need to be im-

proved by adjusting the thresholds. The QoS of this scheme has been changed.

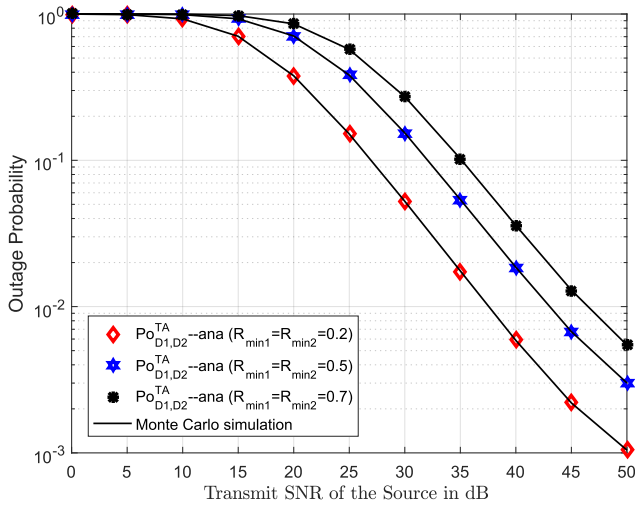


**Fig. 6:** The outage probability of CR-NOMA scheme using a TA on  $R_{\min 1} = R_{\min 2} = \{0.2, 0.5, 0.7\}$ .

Due to the influence of target rate on outage performance, each scheme achieves the different performance and such performance gap changes linearly with the varying transmit SNR at the source (see Fig. 6). It can be noticed that higher target rate leads to worse outage performance.

In Fig. 7, we analyzed the system throughput of the TA scheme with different thresholds  $R_{\min 1} = R_{\min 2} = \{0.2, 0.5, 0.7\}$ . In Fig. 7, the throughput results of the users with the threshold  $R_{\min 1} = R_{\min 2} = 0.2$  have the best performance at low SNRs. The cause is the users have the best outage probability results with  $R_{\min 1} = R_{\min 2} = 0.2$  as showed in Fig. 6. In addition, by increasing SNRs from 25 dB or higher, the throughput results of the users in the proposed models also

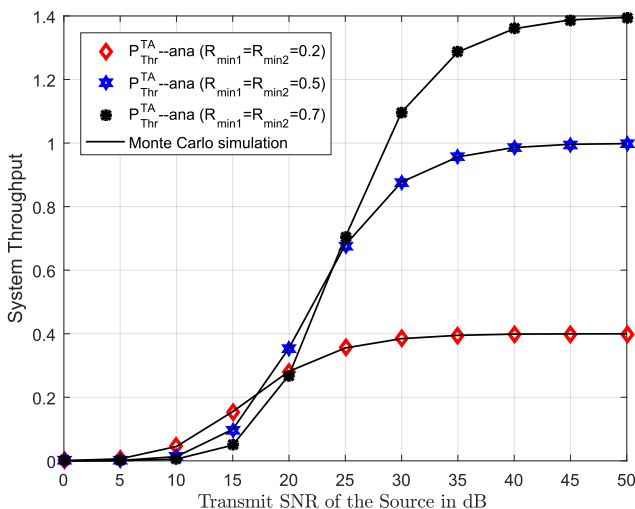


**Fig. 7:** The throughput of CR-NOMA with TA on different target rates.

increased to a corresponding SNRs level, which was gradually reduced  $R_{\min 1} = R_{\min 2} = \{0.7, 0.5, 0.2\}$ , in order.

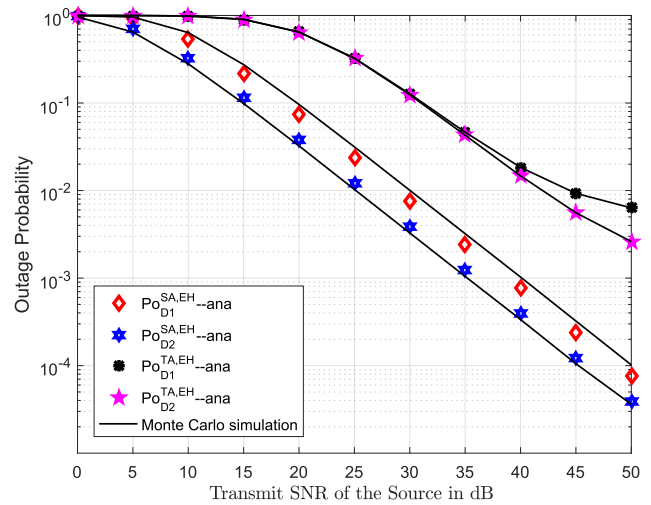


**Fig. 8:** The compared outage probability of CR-NOMA with SA and EH versus TA and EH scheme.

To demonstrate the performance of the TA with EH and SA with EH schemes, we investigated outage probability results for users in the considered CR-NOMA with following parameters: power allocation factor are ( $\alpha_S = \Delta_{R1} = 0.2, \beta_S = \Delta_{R2} = 0.8$ ) and the bit rate threshold is  $0.5 \text{ b}\cdot\text{s}^{-1}\cdot\text{Hz}^{-1}$ . The results show that the proposed energy harvesting for the users  $PD1$  and  $SD2$  in such NOMA scheme can dramatically improve the outage performance with higher power allocation. In case of more power allocated for the NOMA energy harvested user, the outage performance of NOMA is also gradually decreased. The results also showed that the performance curves for simulation and analysis in each scheme are matching.

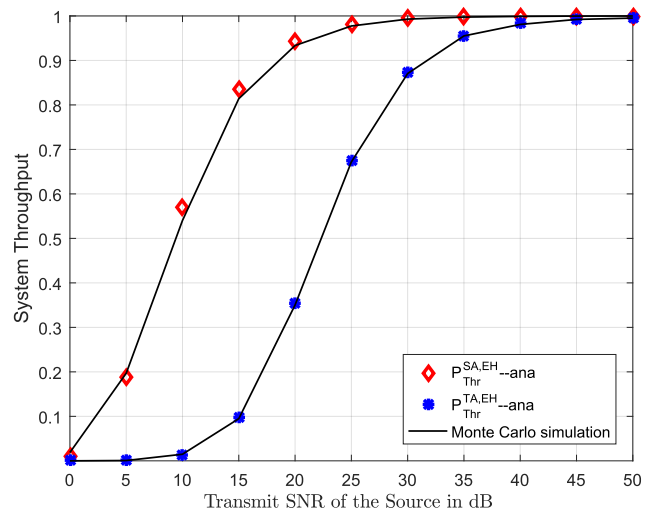


**Fig. 9:** The throughput of CR-NOMA on TA with EH, and SA with EH schemes.

Figure 9 showed the comparison of the system throughput result of the user on TA with EH, and SA with EH schemes as applying energy harvesting for  $PD1$  and  $SD2$ . In this investigation, the  $PR1$  and  $SR2$  used only a part of 100 % of the transmit power that were denoted  $\Delta_{R1}$  and  $\Delta_{R2}$  for second hop transmission. The results of the users in these schemes still achieve throughput performance as solid line and hexagram maker in Fig. 7 on  $R_{\min 1} = R_{\min 2} = 0.5 \text{ b}\cdot\text{s}^{-1}\cdot\text{Hz}^{-1}$ . The results show that even though the  $PR1$  and  $SR2$  do not need to use 100 % power, they still guarantee service quality to the users. That means the users not only are served with good quality but also are supplied power to charge the battery.

## 5. Conclusion

In this investigation, we suggested a novel scheme using CR-NOMA and derived the closed-form expressions of the outage probability and throughput, especially in evaluation of impact of full-duplex relay scheme. By means of numerical results, it is confirmed that our proposed scheme provides design for CR-NOMA with SA is significantly enhanced compared with the CR-NOMA using TA. In addition, impact of wireless energy harvesting to NOMA with the suggested scheme has been analysed, which offers comprehensive design of CR-NOMA system in the future.

## References

- [1] ZHU, H. and J. WANG. Chunk-based resource allocation in OFDMA systems - part I: chunk allocation. *IEEE Transactions on Communications*. 2009, vol. 57, iss. 9, pp. 2734–2744. ISSN 0090-6778. DOI: 10.1109/TCOMM.2009.09.080067.
- [2] BENJEBBOUR, A., Y. SAITO, Y. KISHIYAMA, A. LI, A. HARADA and T. NAKAMURA. Concept and practical considerations of non-orthogonal multiple access (NOMA) for future radio access. In: *International Symposium on Intelligent Signal Processing and Communication Systems*. Naha: IEEE, 2013, pp. 770–774. ISBN 978-1-4673-6361-7. DOI: 10.1109/IS-PACS.2013.6704653.
- [3] TSE, D. and P. WISVANATH. *Fundamentals of Wireless Communication*. Cambridge: Cambridge University Press, 2005. ISBN 978-0511807213.
- [4] ZHANG, R. and L. HANZO. A Unified Treatment of Superposition Coding Aided Communications: Theory and Practice. *IEEE Communications Surveys & Tutorials*. 2011, vol. 13, iss. 3, pp. 503–520. ISSN 1553-877X. DOI: 10.1109/SURV.2011.061610.00102.
- [5] DO, D.-T. and H.-S. NGUYEN. A tractable approach to analyzing the energy-aware two-way relaying networks in the presence of co-channel interference. *EURASIP Journal on Wireless Communications and Networking*. 2016, vol. 2016, iss. 1, pp. 1–10. ISSN 1687-1499. DOI: 10.1186/s13638-016-0777-z.
- [6] NGUYEN, T. N., D.-T. DO, P. T. TRAN and M. VOZNAK. Time Switching for Wireless Communications with Full-Duplex Relaying in Imperfect CSI Condition. *KSII Transactions on Internet and Information Systems*. 2016, vol. 10, no. 9, pp. 4223–4239. ISSN 1976-7277. DOI: 10.3837/tiis.2016.09.011.
- [7] HANIF, M. F., Z. DING, T. RATNARAJAH and G. K. KARAGIANNIDIS. A Minorization-Maximization Method for Optimizing Sum Rate in the Downlink of Non-Orthogonal Multiple Access Systems. *IEEE Transactions on Signal Processing*. 2016, vol. 64, iss. 1, pp. 76–88. ISSN 1827-6660. ISSN 1053-587X. DOI: 10.1109/TSP.2015.2480042.
- [8] NGUYEN, X.-X. and D.-T. DO. Maximum harvested energy policy in full-duplex relaying networks with SWIP. *International Journal of Communication Systems*. 2017, vol. 30, no. 17, pp. 1–16. ISSN 1099-1131. DOI: 10.1002/dac.3359.
- [9] DO, D.-T., H.-S. NGUYEN, M. VOZNAK and T.-S. NGUYEN. Wireless Powered Relaying Networks Under Imperfect Channel State Information: System Performance and Optimal Policy for Instantaneous Rate. *Radioengineering*. 2017, vol. 26, no. 3, pp. 869–877. ISSN 1210-2512. DOI: 10.13164/re.2017.0869.
- [10] NGUYEN, K.-T., D.-T. DO, X.-X. NGUYEN, N.-T. NGUYEN and D.-H. HA. Wireless Information and Power Transfer for Full Duplex Relaying Networks: Performance Analysis. In: *AETA 2015: Recent Advances in Electrical Engineering and Related Sciences*. Ho Chi Minh City: LNEE, 2015, pp. 53–62. ISBN 978-3-319-27245-0. DOI: 10.1007/978-3-319-27247-4.
- [11] LIU, Y., Z. DING, M. ELKASHLAN and H. V. POOR. Cooperative Non-orthogonal Multiple Access With Simultaneous Wireless Information and Power Transfer. *IEEE Journal on Selected Areas in Communications*. 2016, vol. 34, iss. 4, pp. 938–953. ISSN 0733-8716. DOI: 10.1109/JSAC.2016.2549378.
- [12] YU, Y., H. CHEN, Y. LI, Z. DING and L. ZHUO. Antenna Selection in MIMO Cognitive Radio-Inspired NOMA Systems. *IEEE Communications Letters*. 2017, vol. 21,



- iss. 12, pp. 2658–2661. ISSN 1089-7798. DOI: 10.1109/LCOMM.2017.2750153.
- [13] LIU, Y., G. PAN, H. ZHANG and M. SONG. On the Capacity Comparison Between MIMO-NOMA and MIMO-OMA. *IEEE Access*. 2016, vol. 4, iss. 1, pp. 2123–2129. ISSN 2169-3536. DOI: 10.1109/ACCESS.2016.2563462.
- [14] DHUNGAN, Y. and C. TELLAMBURA. Outage probability of underlay cognitive relay networks with spatially random nodes. In: *Global Communications Conference*. Austin: IEEE, 2014, pp. 3597–3602. ISBN 978-1-4799-3512-3. DOI: 10.1109/GLOCOM.2014.7037366.
- [15] YANG, Z., Z. DING, P. FAN and N. AL-DHAHIR. The Impact of Power Allocation on Cooperative Non-orthogonal Multiple Access Networks With SWIPT. *IEEE Transactions on Wireless Communications*. 2017, vol. 16, iss. 7, pp. 4332–4343. ISSN 1536-1276. DOI: 10.1109/TWC.2017.2697380.
- [16] SAITO, Y., Y. KISHIYAMA, A. BENJEBBOUR, T. NAKAMURA, A. LI and K. HIGUCHI. Non-Orthogonal Multiple Access (NOMA) for Cellular Future Radio Access. In: *77th Vehicular Technology Conference*. Dresden: IEEE, 2013, pp. 1–5. ISBN 978-1-4673-6337-2. DOI: 10.1109/VTC-Spring.2013.6692652.
- Military Technical Academy (MTA) in 2014. He works in the Faculty of Electronics and Telecommunications, Sai Gon University, Ho Chi Minh city, Vietnam. He is currently pursuing his Ph.D. degree in Electrical Engineering at VSB–Technical University of Ostrava, Czech Republic. His major interests are in NOMA, energy harvesting, cognitive radio, and physical layer security.
- Dinh-Thuan DO** (Corresponding author) received the B.Sc. degree, M.Eng. degree, and Ph.D. degree from Vietnam National University (VNU-HCMC) in 2003, 2007, and 2013 respectively, all in Communications Engineering. He was a visiting Ph.D. student with Communications Engineering Institute, National Tsing Hua University, Taiwan from 2009 to 2010. Prior joining Ton Duc Thang University, he was a senior engineer at the VinaPhone Mobile Network from 2003 to 2009. Dr. Thuan was recipient of Golden Globe Award from Vietnam Ministry of Science and Technology in 2015. His research interests include signal processing in wireless communications network, NOMA, full-duplex transmission and energy harvesting. He is member of Board of Editors in 3 SCOPUS-indexed journals.
- Miroslav VOZNAK** is Full Professor with Department of Telecommunications, VSB–Technical University of Ostrava. He is currently at the VSB–Technical University of Ostrava. His professional knowledge covers Information and Communication technology. In his research, he deals with wireless networks, Voice over IP, IoT, big data. He is IEEE Senior member and served as Chair of various international conferences.

## About Authors

**Thanh-Nam TRAN** was born in Vinh Long province, Vietnam. He received his M.Sc. from

# Appendix A

## Proof of Proposition 1

We can compute the outage probability for  $D1$  by using TA scheme as below:

$$\begin{aligned}
 P_{O,D1}^{TA} &= 1 - P_{D1}^{TA} = 1 - \Pr(\min\{R_{R1,M1}^{TA}, R_{D1}^{TA}\} > R_{\min 1} \wedge \min\{R_{R1,M2}^{TA}, R_{R2,M2}^{TA}\} > R_{\min 2}) \\
 &= 1 - \Pr\left(\min\left(\underbrace{|h_{S,R1}|^2 \geq \frac{\chi_1(|h_{LI,R1}|^2 \omega_{R1} \rho_{R1} + 1)}{\alpha_S \rho_S}}_{Q_1}, \underbrace{|h_{S,R1}|^2 \geq \frac{\chi_2(|h_{LI,R1}|^2 \omega_{R1} \rho_{R1} + 1)}{(\beta_S - \chi_2 \alpha_S) \rho_S}}_{Q_3}\right)\right) \\
 &\quad \Pr\left(\underbrace{|h_{R1,D1}|^2 \geq \frac{\chi_1}{\epsilon_{R1} \rho_{R1}}}_{Q_2}\right) \Pr\left(\underbrace{|h_{S,R2}|^2 \geq \frac{\chi_2(|h_{LI,R2}|^2 \omega_{R2} \rho_{R2} + 1)}{(\beta_S - \chi_2 \alpha_S) \rho_S}}_{Q_4}\right) \\
 &= 1 - (\min\{Q_1, Q_3\})(Q_2)(Q_4).
 \end{aligned}$$

Following several computation steps as below, Proposition 1 can be proved completely:

$$\begin{aligned}
 Q_1 &= \Pr\left\{|h_{S,R1}|^2 \geq \frac{\chi_1(|h_{LI,R1}|^2 \omega_{R1} \rho_{R1} + 1)}{\alpha_S \rho_S}\right\} = \int_0^{+\infty} \int_{\frac{\chi_1(\omega_{R1} \rho_{R1} y + 1)}{\alpha_S \rho_S}}^{+\infty} f_{|h_{S,R1}|^2}(x) f_{|h_{LI,R1}|^2}(y) dx dy \\
 &= \frac{1}{\sigma_{h_{S,R1}}^2 \sigma_{h_{LI,R1}}^2} \int_0^{+\infty} \int_{\frac{\chi_1(\omega_{R1} \rho_{R1} y + 1)}{\alpha_S \rho_S}}^{+\infty} e^{-\left(\frac{x}{\sigma_{h_{S,R1}}^2} + \frac{y}{\sigma_{h_{LI,R1}}^2}\right)} dx dy = e^{-\left(\frac{\chi_1}{\psi_1}\right)} \frac{\psi_1}{\psi_1 + \chi_1 \omega_{R1} \rho_{R1} \sigma_{h_{LI,R1}}^2},
 \end{aligned}$$

where  $\psi_1 = \alpha_S \rho_S \sigma_{h_{S,R1}}^2$  and  $\chi_1 = 2^{2R_{\min 1}} - 1$ ,

$$Q_2 = \Pr\left\{|h_{R1,D1}|^2 \geq \frac{\chi_1}{\epsilon_{R1} \rho_{R1}}\right\} = \int_{\frac{\chi_1}{\epsilon_{R1} \rho_{R1}}}^{+\infty} f_{|h_{R1,D1}|^2}(x) dx = \int_{\frac{\chi_1}{\epsilon_{R1} \rho_{R1}}}^{+\infty} \frac{1}{\sigma_{h_{R1,D1}}^2} e^{-\frac{x}{\sigma_{h_{R1,D1}}^2}} dx \triangleq e^{-\left(\frac{\chi_1}{\epsilon_{R1} \rho_{R1} \sigma_{h_{R1,D1}}^2}\right)},$$

where  $\epsilon_{R1} = \omega_{R1} = 1$  if relay uses 100 % of the transmit power or  $\epsilon_{R1} = \Delta_{R1} = \alpha_S$  if relay does not use 100 % of the transmit power.

Similarly, we can obtain

$$\begin{aligned}
 Q_3 &= \Pr\left\{|h_{S,R1}|^2 \geq \frac{\chi_2(|h_{LI,R1}|^2 \omega_{R1} \rho_{R1} + 1)}{(\beta_S - \chi_2 \alpha_S) \rho_S}\right\} = \int_0^{+\infty} \int_{\frac{\chi_2(\omega_{R1} \rho_{R1} y + 1)}{(\beta_S - \chi_2 \alpha_S) \rho_S}}^{+\infty} f_{|h_{S,R1}|^2}(x) f_{|h_{LI,R1}|^2}(y) dx dy \\
 &= \int_0^{+\infty} \int_{\frac{\chi_2(\omega_{R1} \rho_{R1} y + 1)}{(\beta_S - \chi_2 \alpha_S) \rho_S}}^{+\infty} \frac{1}{\sigma_{h_{S,R1}}^2} e^{-\frac{x}{\sigma_{h_{S,R1}}^2}} \frac{1}{\sigma_{h_{LI,R1}}^2} e^{-\frac{y}{\sigma_{h_{LI,R1}}^2}} dx dy = e^{-\left(\frac{\chi_2}{\psi_3}\right)} \frac{\psi_3}{\psi_3 + \chi_2 \omega_{R1} \rho_{R1} \sigma_{h_{LI,R1}}^2},
 \end{aligned}$$

where  $\psi_3 = (\beta_S - \chi_2 \alpha_S) \rho_S \sigma_{h_{S,R1}}^2$  and  $\chi_2 = 2^{2R_{\min 2}} - 1$ .

Next, we compute

$$\begin{aligned}
 Q_3 &= \Pr\left\{|h_{S,R2}|^2 \geq \frac{\chi_2(|h_{LI,R2}|^2 \omega_{R2} \rho_{R2} + 1)}{(\beta_S - \chi_2 \alpha_S) \rho_S}\right\} = \int_0^{+\infty} \int_{\frac{\chi_2(\omega_{R2} \rho_{R2} y + 1)}{(\beta_S - \chi_2 \alpha_S) \rho_S}}^{+\infty} f_{|h_{S,R2}|^2}(x) f_{|h_{LI,R2}|^2}(y) dx dy \\
 &= e^{-\left(\frac{\chi_2}{\psi_4}\right)} \frac{\psi_4}{\psi_4 + \chi_2 \omega_{R2} \rho_{R2} \sigma_{h_{LI,R2}}^2},
 \end{aligned}$$

where  $\psi_4 = (\beta_S - \chi_2\alpha_S) \rho_S \sigma_{h_{S,R2}}^2$ .

$$Q_5 = \Pr \left\{ |h_{R2,D2}|^2 \geq \frac{\chi_2}{\epsilon_{R2}\rho_{R2}} \right\} = \int_{\frac{\chi_2}{\epsilon_{R2}\rho_{R2}}}^{+\infty} f_{|h_{R2,D2}|^2}(x) dx \triangleq e^{-\left(\frac{\chi_2}{\epsilon_{R2}\rho_{R2}\sigma_{h_{R2,D2}}^2}\right)},$$

where  $\epsilon_{R2} = \omega_{R2} = 1$  if relay uses 100 % of the transmit power or  $\epsilon_{R2} = \Delta_{R2} = \beta_S$  if relay does not use 100 % of the transmit power.

Similarly, we can compute outage event for  $D2$  as below:

$$\begin{aligned} P_{O,D2}^{TA} &= 1 - P_{D2}^{TA} = 1 - \Pr (R_{R1,M1}^{TA} > R_{\min 1} \wedge \min \{R_{R1,M2}^{TA}, R_{R2,M2}^{TA}, R_{D2}^{TA}\} > R_{\min 2}) \\ &= 1 - \Pr \left( \min \left( \underbrace{|h_{S,R1}|^2 \geq \frac{\chi_1 (|h_{LI,R1}|^2 \omega_{R1}\rho_{R1} + 1)}{\alpha_S \rho_S}}_{Q_1}, \underbrace{|h_{S,R1}|^2 \geq \frac{\chi_2 (|h_{LI,R1}|^2 \omega_{R1}\rho_{R1} + 1)}{(\beta_S - \chi_2\alpha_S) \rho_S}}_{Q_3} \right) \right) \\ &\Pr \left( \underbrace{|h_{S,R2}|^2 \geq \frac{\chi_2 (|h_{LI,R2}|^2 \omega_{R2}\rho_{R2} + 1)}{(\beta_S - \chi_2\alpha_S) \rho_S}}_{Q_4} \right) \Pr \left( \underbrace{|h_{R2,D2}|^2 \geq \frac{\chi_2}{\epsilon_{R2}\rho_{R2}}}_{Q_5} \right) \\ &= 1 - (\min \{Q_1, Q_3\}) (Q_4) (Q_5). \end{aligned}$$

It is worth noting that  $Q_1, Q_3, Q_4,$  and  $Q_5$  can be obtained in previous section.

## Appendix B Proof of Proposition 2

To prove Proposition 2, the outage probability can be re-written as

$$\begin{aligned} P_{O,D1}^{SA} &= 1 - P_{D1}^{SA} = 1 - \Pr (\min \{R_{R1,M1}^{SA}, R_{D1}^{SA}\} > R_{\min 1} \wedge \min \{R_{R1,M2}^{SA}, R_{R2,M2}^{SA}\} > R_{\min 2}) \\ &= 1 - \Pr \left( \min \left( \underbrace{|h_{S,R1}|^2 \geq \frac{\chi_1}{\alpha_S \rho_S}}_{Q'_1}, \underbrace{|h_{S,R1}|^2 \geq \frac{\chi_2 (|h_{LI,R1}|^2 \omega_{R1}\rho_{R1} + 1)}{(\beta_S - \chi_2\alpha_S) \rho_S}}_{Q'_3} \right) \right) \\ &\Pr \left( \underbrace{|h_{R1,D1}|^2 \geq \frac{\chi_1}{\epsilon_{R1}\rho_{R1}}}_{Q'_2} \right) \Pr \left( \underbrace{|h_{S,R2}|^2 \geq \frac{\chi_2}{(\beta_S - \chi_2\alpha_S) \rho_S}}_{Q'_4} \right) \\ &= 1 - (\min \{Q'_1, Q'_3\}) (Q'_2) (Q'_4). \end{aligned}$$

Similarly, the probability for SD2 in SA mode can be defined as follows:

$$\begin{aligned}
 P_{O,D2}^{SA} &= 1 - P_{D2}^{SA} = 1 - \Pr(R_{R1,M1}^{SA} > R_{\min 1} \wedge \min\{R_{R1,M2}^{SA}, R_{R2,M2}^{SA}, R_{D2}^{SA}\} > R_{\min 2}) \\
 &= 1 - \Pr\left(\min\left(\underbrace{|h_{S,R1}|^2 \geq \frac{\chi_1}{\alpha_S \rho_S}}_{Q'_1}, \underbrace{|h_{S,R1}|^2 \geq \frac{\chi_2}{(\beta_S - \chi_2 \alpha_S) \rho_S}}_{Q'_3}\right)\right) \\
 &\quad \Pr\left(\underbrace{|h_{S,R2}|^2 \geq \frac{\chi_2}{(\beta_S - \chi_2 \alpha_S) \rho_S}}_{Q'_4}\right) \Pr\left(\underbrace{|h_{R2,D2}|^2 \geq \frac{\chi_2}{\epsilon_{R2} \rho_{R2}}}_{Q'_5}\right) \\
 &= 1 - (\min\{Q'_1, Q'_3\}) (Q'_4) (Q'_5).
 \end{aligned}$$

It is important to notice that the computations for  $Q'_1, Q'_2, Q'_3, Q'_4,$  and  $Q'_5$  can be solved similarly as in proof of **Proposition 1**.

This is the end of the proof.